Modeling Emergence in Neuroprotective Regulatory Networks

Antonio P. Sanfilippo[1], Jereme N. Haack[1], Jason E. McDermott[1], Susan L. Stevens[2], and Mary P. Stenzel-Poore[2]

[1] Pacific Northwest National Laboratory, Richland, WA, USA
[2] Oregon Health & Sciences University, Portland, OR, USA
{antonio,jereme,jason.mcdermott}@pnnl.gov,
{stevensu,poorem}@ohsu.ed

Abstract. The use of predictive modeling in the analysis of gene expression data can greatly accelerate the pace of scientific discovery in biomedical research by enabling *in silico* experimentation to test disease triggers and potential drug therapies. Techniques such as agent-based modeling and multi-agent simulations are of particular interest as they support the discovery of emergent pathways, as opposed to other dynamic modeling approaches such as dynamic Bayesian nets and system dynamics. Thus far, emergence-modeling techniques have been primarily applied at the multi-cellular level, or have focused on signaling and metabolic networks. We present an approach where emergence modeling is extended to regulatory networks and demonstrate its application to the discovery of neuroprotective pathways. An initial evaluation of the approach indicates that emergence modeling provides novel insights for the analysis of regulatory networks which can advance the discovery of acute treatments for stroke and other diseases.

Keywords: regulatory networks, emergence, complex systems, agent-based modeling, neuroprotection, stroke.

1 Introduction

Stroke is the third leading cause of death and the major cause of disability in the United States. Each year, approximately 795,000 people suffer a stroke, and more than 140,000 die; those who survive are subject to recurrent attacks and long-term disability [1]. Injury due to ischemic stroke occurs as a result of a sequence of events that involve complex interactions across fundamental cell injury mechanisms. The potential for neuroprotective stroke therapy through agents that interfere in the ischemic cascade of cell injury is therefore enormous.

Preclinical evaluations of neuroprotectants have fostered high expectations of clinical efficacy and a large number of neuroprotective agents have been designed to interrupt the ischemic cascade. However, neuroprotective clinical trials run over the past 30 years have failed to provide a strategy to improve outcome after acute ischemic stroke. A 2006 review of 1026 experimental treatments in acute stroke

K. Glass et al. (Eds.): COMPLEX 2012, LNICST 126, pp. 291–302, 2013.

revealed that no particular drug mechanism taken forward to clinical trial has shown superior efficacy in animal models of focal ischemia [2]. These conclusions are corroborated by more recent studies [3-5]. New approaches to stroke neuroprotection are needed to break this impasse. Dynamic modeling approaches such as agent-based modeling have great potential in providing new ways of understanding neuronal ischemic injury as they support an active systems-biology analytical framework through the discovery of emergent pathways in complex biological systems. The goal of this paper is to explore and evaluate the use of agent-based modeling for the discovery of emergent neuroprotective pathways in regulatory networks.

2 Background

A major weakness in current neuroprotective approaches to stroke therapy is due to a poor understanding of the complexity of interconnections across molecular pathways induced in brain cells by ischemia. For example, [2] observe that current approaches to stroke therapy tend to frame drug activity exclusively in terms of the dominant schema of stroke damage (e.g. excitotoxicity, free radical damage). The failure of these approaches may "reflect the multifaceted nature of the sequelae of ischemic stroke" [2, p.474]. A dynamic network analysis of ischemic stroke that provides an active systems biology framework for understanding neuronal ischemic injury would therefore be better suited to address the complexity of ischemic stroke. Agent-based modeling techniques are of great interest in this regards as they support the discovery of emergent pathways in complex biological systems. The focus on modeling emergence is of particular interest as it supports the discovery of new network pathways that emerge iteratively from self-organizational properties of gene and gene clusters, as opposed to other dynamic modeling approaches such as dynamic Bayesian nets and system dynamics where network structure remains unchanged through the simulation process.

In systems biology research, agent-based and multi-agent simulations have been primarily applied at the multi-cellular level to study topics such as tumor growth [6, 7] and immune responses [8, 9]. At the molecular level, agent-based modeling efforts have focused on signaling networks [10, 11, 12] and metabolic networks [13]. So far, most modeling work on regulatory networks has relied on algorithms other than agent-based modeling [14, 15].

3 Data Selection and Network Creation

During the last decade, substantial effort has been devoted to understanding the systems biology of neuroprotection in stroke by researching the effect of preconditioning on the genomic response to cerebral ischemia [16, 17]. This work has yielded rich gene expression data that provides evidence about the genomic dynamics of neuroprotection in diverse contexts and can be used to train dynamic pathway models of neuroprotection in stroke. We use the gene expression data generated by these studies as our point of departure. These consist of microarray results from blood of mice in a transcriptional study of a mouse model of preconditioning-induced

neuroprotection against stroke injury [18]. The dataset comprises five treatments: ischemic preconditioning; lipopolysaccharide (LPS) injection; CpG injection, and two control treatments (saline injection and sham surgery). Microarray data were taken at 3, 24 and 72 hours post treatment, and 3 and 24 hours post-stroke. We focus on the two drug treatments documented in these data: LPS and CpG injection.

We selected 7352 significant gene probes from the dataset described in [18] (see previous paragraph) using the normalized probe intensities obtained with the robust multi-array average algorithm [19] to evaluate significantly changing probes, and filtering for p-value < 0.05 and fold changes greater than 2.0 compared to a baseline group. Next, we identified 25 functional gene modules encompassing the selected 7352 gene probes using hierarchical clustering, as shown in Figure 1. We then applied a modified version of the *Inferelator* algorithm [20] to learn ordinary differential equations (ODEs) between clusters. This algorithm uses an approach called L1 error regression (also known as "lasso") to choose a parsimonious set of regulatory influences that can model the expression of each cluster [21, 22]. The relation between the expression of a target (y) and the expression levels of regulators with non-null influences on y (X) is expressed by the equation in (1), where τ is the time step used in model construction, and β is the weight for relationship X on y, as determined by L_1 shrinkage using least angle regression [22]. This process as a whole yields the network model in Figure 1, where the expression of a target cluster can be predicted given the expression levels of the input regulatory clusters linked to the target cluster. Details of this work are provided in [23].

$$\tau \frac{dy}{dt} = -y + \sum \beta_j X_j \tag{1}$$

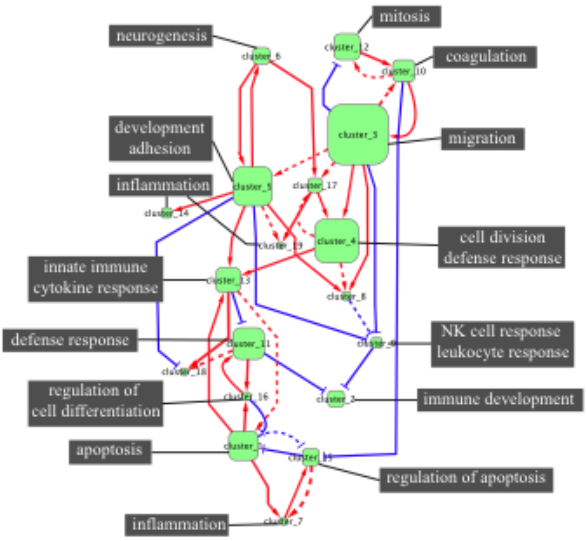

Fig. 1. Regulatory influence network model of neuroprotection in ischemia

We used simulated annealing to optimize the ODEs between clusters. Simulated annealing randomly perturbs variables in the model, then compares the performance of the perturbed model with the original using a fitness function. Perturbations that improve performance are retained in the model and perturbations that decrease performance can be retained based on a probability that is decreased over the simulation, resulting in more and more conservative changes to the model. We used a fitness function to evaluate the performance of each test matrix by the correlation of its simulated expression values with the observed expression values. The optimized ODEs yield a high correlation coefficient between the observed and simulated cluster connections (about 0.8). For further details of this work see [24].

4 Modeling Emergent Neuroprotective Regulatory Networks

Our hypothesis is that neuroprotective biological networks emerge from self-organizational regulatory properties of genes, akin to how complex systems arise in nature from swarming behaviors – e.g. food source selection and cooperative transport in ant colonies, hive construction in termites, formation of slime mold colonies [25]. More specifically, genes or functional gene clusters may be systemically driven to form new pathway connections during an ischemic event driven by a systemic push to maintain their expression values at levels that characterize a healthy organism. The neuroprotective pathways emerging from these gene networking activities may be enabled by specific treatments such as LPS or CpG injection. To test this hypothesis, we developed agent-based models (ABM) for two drug treatments in the data described in [18], LPS and CpG, using the functional clusters and ODEs in [23, 24], and then computed the correlation coefficient between the models' simulations and the observed data.

For each treatment in our dataset (LPS and CpG), there is a set of weights $\{W_1,\ldots,W_n\}$ from solved ODEs in the optimized Inferrelator model across gene clusters $\{C_1,\ldots,C_{25}\}$ (see previous section and [24]), as shown in Table 1. Each weight specifies how the expression level of a cluster varies as a function of being connected to another cluster. Each cluster has a set of expressions values {E1,…,En}, for each treatment; each Ej is the expression value of the cluster at the time point at which microarray data were taken – e.g. 3 and 72 hours post-treatment, and 3 hours post-stroke (hour 75) – as shown in Table 2. When clusters C_i and C_j are linked at time T_k, indicated as $C_i \rightarrow^{Tk} C_j$, the expression value of C_i is calculated as shown in (2) where:

- $E_{Ci\rightarrow}{}^{Tk}{}_{Cj}$ is the expression value of C_i at time T_k, when C_i is linked to C_j
- E_{CiTk} is the expression value of C_i at time T_k
- E_{CjTk} is the expression value of C_j at time T_k
- $W_{Ci\rightarrow}{}^{Tk}{}_{Cj}$ is the weight relating C_i and C_j at time T_k.

$$E_{Ci\rightarrow}{}^{Tk}{}_{Cj} = E_{CiTk} + (E_{CjTk} * W_{Ci\rightarrow}{}^{Tk}{}_{Cj}) \quad (2)$$

For example, the expression value of **cluster_1** when linking to **cluster_3** at hour 3 (*H3*) is calculated as shown in (3). The model uses the equation in (2) to calculate the expression value of each cluster in the simulation process.

$$E_{C1\rightarrow}{}^{H3}{}_{C3} = -1.486 + (1.686 * -0.738) = -2.730 \quad (3)$$

Table 1. Weights relating gene cluster (LPS treatment)

	cluster_1	***cluster_2***	***cluster_3***	**…**
cluster_1	0.124	0	−0.738	…
cluster_2	−0.032	0	−0.283	…
cluster_3	−0.060	0	−0.197	…
…	…	…	…	…

Table 2. Cluster expression levels by time point (LPS treatment)

	Hour 3	***Hour 72***	***Hour 75***	**…**
cluster_1	−1.486	0.034	−0.738	…
cluster_3	1.686	0.500	1.573	
…	…	…	…	…

In the agent-based model we have developed, the post-stroke gene-cluster network (hour 75, 3 hour post-stroke) provides the initial network state for the simulation. The expression values of the clusters in pre-stroke network (hour 72) provide the target "healthy" expression values that the clusters in the post-stroke network try to achieve. The objective of the simulation is to observe how the system behaves post-stroke in terms of forming regulatory gene networks that offer neuroprotection with reference to two treatments, LPS and CpG injection.

At every simulation tick, each cluster whose expression value is different from the target "healthy" expression value, attempts to improve its expression value by selecting a cluster to link up to at random. If the new expression value for the cluster, calculated as shown in (1), is closer to the target expression value, then it is used to replace the old expression value for the cluster; otherwise, it is rejected. A steady state in the simulation is reached when either all clusters achieve their target "healthy" expression values, or when clusters can no longer improve their expression values by establishing new network connections.

We used NetLogo [25] to implement the agent-based model that simulates the neuroprotective dynamics of the post-stroke regulatory network. Figure 2 provides a graphical description of the simulation environment with reference to the simulated LPS neuroprotective network dynamics. The left quadrant contains the clusters in the initial network state. The center quadrant represents the steady state of the cluster network that emerges through simulation. Shades of color from red to green indicate how close a cluster's expression value is to the target expression value. Green indicates that the post-stroke and target clusters' expression are the same. Red indicates that the post-stroke and target clusters' expression are as far apart as they

can be. At each simulation tick, clusters can establish or remove links with other clusters. The number of clusters connections added (blue) and removed (red) is represented in the "Connection" graph window (top right). As new links are added and old ones removed, the clusters can come closer to or further from the target expression value, as indicated by the "good-bad" black line in the "Gene Status" graph. As they do so, the clusters' expression levels change, as indicated by the "exp-change" blue line in the "Gene Status" graph window (bottom right). When there is no more change (i.e. the "exp-change" blue line in the "Gene Status" graph goes down to 0), the simulation reaches a steady state. In the simulation shown in Figure 2, the system reaches a steady state after establishing 201 connections, in approximately one thousand simulation ticks. Given the nature of the randomness of the way cluster interact establishing or severing network connections, rerunning a simulation is unlikely to yield the same network. This variation provides a rich set of alternative neuroprotective scenarios that are possible from the same network premises.

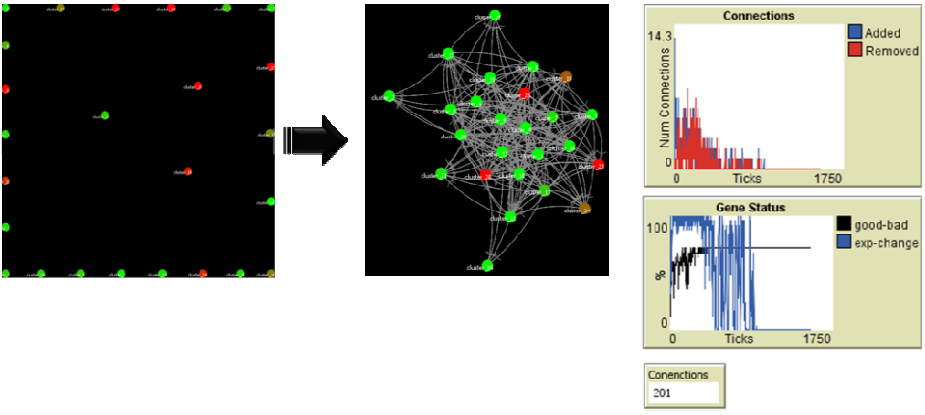

Fig. 2. LPS neuroprotective regulatory network simulation in NetLogo

5 Results and Evaluation

We run two simulations, one for each of the two treatments targeted for exploration: LPS and CpG injection. To assess the validity of the simulations generated, we correlated the predicted expression values of the 25 clusters from the simulation results with the observed expression values of the 25 clusters in the dataset at 24 hours post-stroke. We also established 25 different baseline simulation results by randomizing weight values in the input matrix of cluster to cluster weights (see Table 1). Each set of baseline simulation results included some 10,000 ticks/iterations. The rationale in using a baseline with random weight values is to verify that "real" correlation results obtained with the non-random weights are significantly better than results obtained by chance.

Figure 3 shows the correlation coefficients of real and randomized simulation results with observed expression values for the LPS treatment. The mean correlation coefficient for the real simulation (e.g. averages across the 25 clusters) is 0.76 while the mean correlation coefficient for the 25 sets of randomized simulation results is

0.22, with a p-value below 2.2e-16. These results provide a clear indication that our model generates simulations for the LPS treatment that have a significant correlation with observed data and are not due to chance.

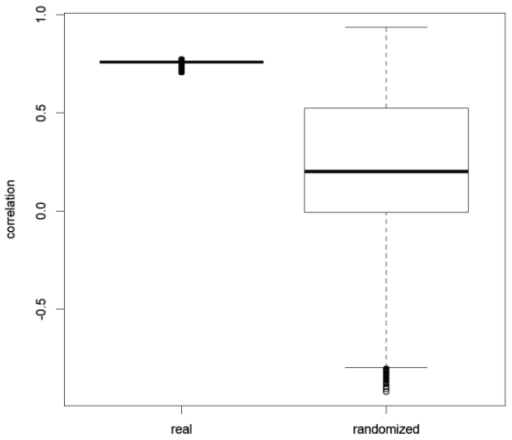

Fig. 3. Correlation coefficient of real and randomized simulation results with observed expression values for LPS treatment ($p < 2.2e\text{-}16$)

We also assessed cluster by cluster performance by measuring the distance between predicted (*EP*) and observed (*EO*) cluster expression values as indicated in (4). As shown in Figure 4, while some clusters perform better than others, all predicted and observed cluster expression values aside from cluster 1 are less than 10% apart. Further improvements can be achieved by addressing cluster by cluster performance – e.g. improving the accuracy of the ODEs that provide the weights and/or the ODE optimization algorithm (see section 3).

$$\text{dist}(EP_i, EO_j) = \left|EP_i/(EP_i + EO_j)\right|, \qquad where\ i, j, k, l \geq 1 \tag{4}$$

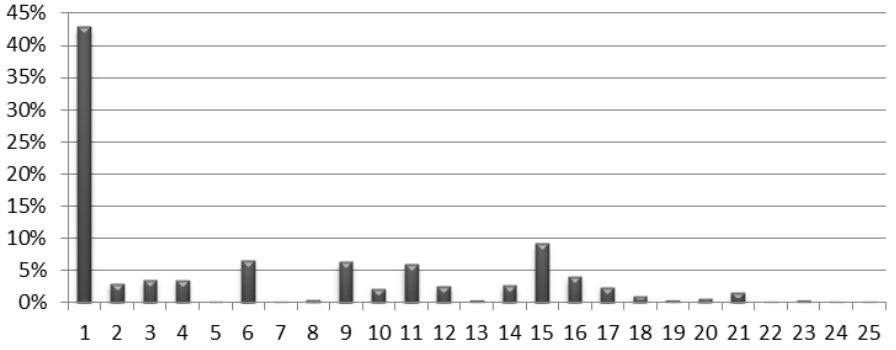

Fig. 4. Cluster by cluster distance between real-simulated and observed expression values for LPS. Distance values have been normalized. 0% indicates perfect fit.

The evaluation of the CpG-treatment simulations corroborates the LPS results, as shown in Figure 5 and 6.

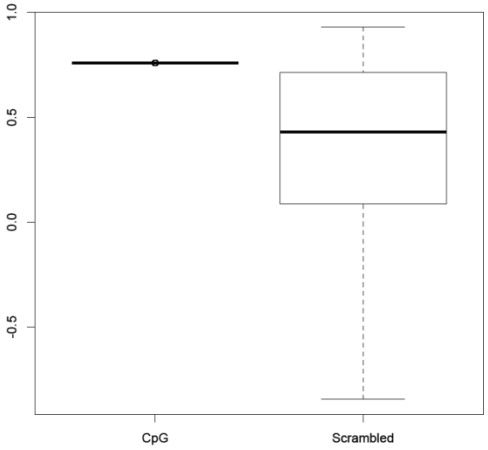

Fig. 5. Correlation coefficient of real and randomized simulation results with observed expression values for CpG treatment ($p < 2.2e-16$)

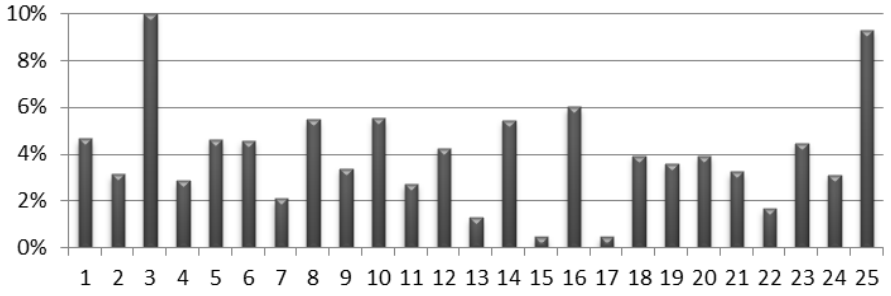

Fig. 6. Cluster by cluster distance between real-simulated and observed expression values for CpG. Distance values have been normalized. 0% indicates perfect fit..

5.1 Validation of Inferred Links across Clusters Using Independent Data Sources

As an additional evaluation measure, we assessed the biological plausibility of cluster links in the simulated networks by verifying that relationships between genes contained in connected clusters were attested in independent data sources. We used four sets of references derived from known gene-interaction databases for verification purposes:

1. Regulatory interactions (regulator to target relationships) derived from CHIP experiments were obtained from the ChEA database [26] giving 2506 edges between 1587 genes included in our model

2. Protein-protein interactions (PPI) were obtained from the Human Proteome Research Database (HPRD) [27], and identifiers were mapped to mouse using gene symbols giving 2974 edges between 1393 genes included in our model. Though some interactions identified in human may not be preserved in mouse, overall they are likely to be consistent across organisms [28]
3. Known gene regulatory interactions (Reg) were obtained from the Molecular Signatures Database [29] giving 1895 edges between 570 genes in our model
4. Functional interactions derived from computational integration of multiple data source (Functional) were obtained from high-confidence (score > 0.5) interactions made by MouseNet [30] giving 2307 edges between 1023 genes in our model.

For each cluster in our model, we determined the number of known interactions (i.e. those attested in the four databases described above) between a gene/gene product in the cluster and genes in each of the other clusters. We used the network model derived through the *Inferelator* algorithm discussed in section 3 (ODE Model) as baseline. The results of this evaluation are shown in Table 3.

We run 30 different simulations with the agent-based model (ABM) described in section 4 using different random seeds so as to maximize the difference across simulation results, and counted the number of times an edge was found between two clusters in all the simulated networks. The model was considered to have a valid edge between two clusters if it occurred in 25 or more simulations. To determine a p-value for the interactions, we counted interactions gathered by randomizing the known edges for each external interaction dataset 1000 times – for undirected edges (HPRD and MouseNet), relationships were counted for both directions. For each interaction dataset, those cluster-to-cluster relationships with a p-value of less than 0.05 were considered to be true positive (TP) matches if there was a corresponding edge in our inferred model, and false positive (FP) matches otherwise. If the p-value was greater than 0.05 and there was no matching inferred edge, we would count a true negative (TN) match; we would count a false negative (FN) match otherwise. Accuracy was calculated as shown in (5).

$$accuracy = \frac{TP + TN}{TP + TN + FP + FN} \tag{5}$$

As shown in Table 3, the results of this evaluation show that the ABM regulatory network models for LPS and CpG are well supported by all independent interaction data sources, and yield a better match than the network model derived through the *Inferalator* algorithm (ODE model). The overlap between inferred and independently documented gene-to-gene links ranges from 67.9% 80.6%. However, if we combine results across each interaction dataset by counting a match as a true positive or true negative if it was validated by any interaction dataset, the combined accuracy is around 90% for both the inferred LPS and CpG models. The number of edges in each of these models at this threshold (considering 25 or more occurrences as an edge) was less than half that in the ODE-based model. This is because using the ABM results we were able to filter the edges based on confidence, as determined by frequency. This

indicates that the ABM is producing accurate interactions, and that the more frequently an edge is seen across simulations, the more accurate it is.

Table 3. Validation of cluster-to-cluster interactions from simulated regulatory networks through comparison with independent data sources. The network model derived through the *Inferalator* algorithm (ODE Model) serves as baseline.

Datasets	ODE Model (baseline)	Agent-Based Model for LPS	Agent-Based Model for CpG
1. CHIP	60.9%	80.6%	79.5%
2. PPI	66.8%	73.1%	74.2%
3. Reg	64.3%	69.0%	67.9%
4. Functional	64.3%	75.6%	76.7%
1-4	82.0%	90.0%	89.8%
Number of network edges	133	50	58

6 Conclusions

The methodology we have described in this paper provides the first step towards using the notion of emergence to model regulatory gene networks. The ensuing approach can be used to uncover novel therapies for a variety of diseases by simulating how protective pathways may endogenously form from a preconditioning stimulus. The specific embodiment presented shows how neuroprotective pathways emerge from preconditioning treatment with LPS and CpG by letting gene clusters search and establish links that maximize proximity to the expression level of a healthy organism. Due to the self-organizational dynamics of the emergent approach to modeling, there are potentially many ways in which neuroprotective regulatory networks may emerge. Therefore, different simulation runs with the same cluster-to-cluster weights, and clusters target and initial expression levels is likely to output different networks. For example, alternative steady states resulting from the same simulation setup shown in Figure 2 may have less/more and different connections, as shown in Figure 7. This variety is of great potential interest in understanding how differently the organism may respond to the same treatment in order to overcome disease.

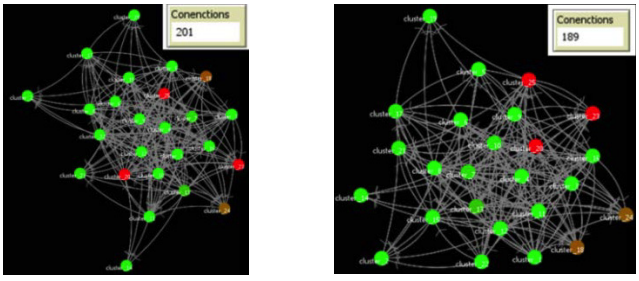

Fig. 7. Alternative simulations of LPS neuroprotective regulatory network

Acknowledgements. The research described in this paper was supported under NIH/NINDS grant R01NS057484-05.

References

1. The Internet Stroke Center, http://www.strokecenter.org/patients/~about-stroke/stroke-statistics (accessed on June 7, 2012)
2. O'Collins, V.E., Macleod, M.R., Donnan, G.A., Horky, L.L., van der Worp, B.H., Howells, D.W.: 1,026 experimental treatments in acute stroke. Ann. Neurol. 59(3), 467–477 (2006)
3. Savitz, S.I.: A critical appraisal of the NXY-059 neuroprotection studies for acute stroke: a need for more rigorous testing of neuroprotective agents in animal models of stroke. Exp. Neurol. 205(1), 20–25 (2007)
4. Fisher, M., Feuerstein, G., Howells, D.W., Hurn, P.D., Kent, T.A., Savitz, S.I., Lo, E.H., STAIR Group: Update of the stroke therapy academic industry roundtable preclinical recommendations. Stroke 40(6), 2244–2250 (2009)
5. Sahota, P., Savitz, S.I.: Investigational therapies for ischemic stroke: neuroprotection and neurorecovery. Neurotherapeutics 8(3), 434–451 (2011)
6. Zhang, L., Athale, C., Deisboeck, T.: Development of a three-dimensional multiscale agent-based tumor model: simulating gene-protein interaction profiles, cell phenotypes and multicellular patterns in brain cancer. J. Theor. Biol. 244(1), 96–107 (2007)
7. Engelberg, J., Ropella, G., Hunt, C.: Essential operating principles for tumor spheroid growth. BMC Syst. Biol. 2(1), 110 (2008)
8. Lollini, P., Motta, S., Pappalardo, F.: Discovery of cancer vaccination protocols with a genetic algorithm driving an agent based simulator. BMC Bioinf. 7(1), 352 (2006)
9. Li, N., Verdolini, K., Clermont, G., Mi, Q., Rubinstein, E., Hebda, P., Vodovotz, Y.: A patient-specific in silico model of inflammation and healing tested in acute vocal fold injury. PLoS ONE 3(7), e2789 (2008)
10. Gonzalez, P., Cardenas, M., Camacho, D., Franyuti, A., Rosas, O., Lagunez-Otero, J.: Cellulat: an agent-based intracellular signalling model. Biosystems 68(2-3), 171–185 (2003)
11. Pogson, M., Smallwood, R., Qwarnstrom, E., Holcombe, M.: Formal agent-based modelling of intracellular chemical interactions. Biosystems 85(1), 37–45 (2006)
12. Pogson, M., Holcombe, M., Smallwood, R., Qwarnstrom, E.: Introducing Spatial Information into Predictive NF- κB Modelling-An Agent-Based Approach. PLoS ONE 3(6), e2367 (2008)
13. Klann, M., Lapin, A., Reuss, M.: Agent-based simulation of reactions in the crowded and structured intracellular environment: Influence of mobility and location of the reactants. BMC Syst. Biol. 5(1), 71 (2011)
14. Schlitt, T., Brazma, A.: Current approaches to gene regulatory network modelling. BMC Bioinf. 8(suppl. 6), S9 (2007)
15. Karlebach, G., Shamir, R.: Modelling and analysis of gene regulatory networks. Nat. Rev. Mol. Cell Biol. 9(10), 770–780 (2008)
16. Stenzel-Poore, M.P., Stevens, S.L., Xiong, Z., Lessov, N.S., Harrington, C.A., Mori, M., Meller, R., Rosenzweig, H.L., Tobar, E., Shaw, T.E., Chu, X., Simon, R.P.: Effect of ischaemic preconditioning on genomic response to cerebral ischaemia: similarity to neuroprotective strategies in hibernation and hypoxia-tolerant states. Lancet 362(9389), 1028–1037 (2003)

17. Stevens, S.L., Ciesielski, T.M., Marsh, B.J., Yang, T., Homen, D.S., Boule, J.L., Lessov, N.S., Simon, R.P., Stenzel-Poore, M.P.: Toll-like receptor 9: a new target of ischemic preconditioning in the brain. J. Cereb. Blood Flow Metab. 28(5), 1040–1047 (2008)
18. Marsh, B., et al.: Systemic lipopolysaccharide protects the brain from ischemic injury by reprogramming the response of the brain to stroke: a critical role for IRF3. J. Neurosci. 29, 9839–9849 (2009)
19. Irizarry, R.A., Hobbs, B., Collin, F., Beazer-Barclay, Y.D., Antonellis, K.J., Scherf, U., Speed, T.P.: Exploration, Normalization, and Summaries of High Density Oligonucleotide Array Probe Level Data. Biostatistics 4(2), 249–264 (2003)
20. Bonneau, R., et al.: The Inferelator: an algorithm for learning parsimonious regulatory networks from systems-biology data sets de novo. Genome Biol. 7, R36 (2006)
21. Efron, B., Johnstone, I., Hastie, T., Tibshirani, R.: Least angle regression. Annals of Statistics 32, 407–499 (2003)
22. Tibshirani, R.: Regression shrinkage and selection via the lasso. J. Royal Statist. Soc. B 58, 267–288 (1996)
23. McDermott, J.E., Archuleta, M., Stevens, S.L., Stenzel-Poore, M.P., Sanfilippo, A.: Defining the players in higher-order networks: predictive modeling for reverse engineering functional influence networks. In: Pac. Symp. Biocomput., pp. 314–325 (2011a)
24. Mcdermott, J., Jarman, K., Taylor, R., Lancaster, M., Stevens, S., Vartanian, K., Stenzel-Poore, M., Sanfilippo, A.: Modeling Cumulative Change of Dynamic Regulatory Processes in Stroke. PLoS Computational Biology (forthcoming)
25. Camazine, S., Deneubourg, J., Franks, N., Sneyd, J., Theraulaz, G., Bonabeau, E.: Self-Organization in Biological Systems. Princeton University Press (2011)
26. Wilensky, U.: NetLogo. Center for Connected Learning and Computer-Based Modeling, Northwestern University, Evanston, IL (1999), `http://ccl.northwestern.edu/netlogo/`
27. Lachmann, A., Xu, H., Krishnan, J., Berger, S.I., Mazloom, A.R., et al.: ChEA: Transcription Factor Regulation Inferred from Integrating Genome-Wide ChIP-X Experiments. Bioinformatics (2010)
28. Peri, S., Navarro, J.D., Kristiansen, T.Z., Amanchy, R., Surendranath, V., et al.: Human protein reference database as a discovery resource for proteomics. Nucleic Acids Res. 32, D497–D501 (2004)
29. Yu, H., Luscombe, N.M., Lu, H.X., Zhu, X., Xia, Y., et al.: Annotation Transfer Between Genomes: Protein-Protein Interologs and Protein-DNA Regulogs. Genome Res. 14, 1107–1118 (2004)
30. Liberzon, A., Subramanian, A., Pinchback, R., Thorvaldsdottir, H., Tamayo, P., et al.: Molecular signatures database (MSigDB) 3.0. Bioinformatics 27, 1739–1740 (2011)
31. Kim, W.K., Krumpelman, C., Marcotte, E.M.: Inferring mouse gene functions from genomic-scale data using a combined functional network/classification strategy. Genome Biology 9(suppl. 1), S5 (2008)